Development 135, 2627-2636 (2008) doi:10.1242/dev.016329

Role for PADI6 and the cytoplasmic lattices in ribosomal storage in oocytes and translational control in the early mouse embryo

Piraye Yurttas[1,2,*], Alejandra M. Vitale[1,*], Robert J. Fitzhenry[1], Leona Cohen-Gould[3], Wenzhu Wu[1], Jan A. Gossen[4] and Scott A. Coonrod[1,†,‡]

The mechanisms that mediate the establishment of totipotency during the egg-to-embryo transition in mammals remain poorly understood. However, it is clear that unique factors stored in the oocyte cytoplasm are crucial for orchestrating this complex cellular transition. The oocyte cytoplasmic lattices (CPLs) have long been predicted to function as a storage form for the maternal contribution of ribosomes to the early embryo. We recently demonstrated that the CPLs cannot be visualized in *Padi6*$^{-/-}$ oocytes and that *Padi6*$^{-/-}$ embryos arrest at the two-cell stage. Here, we present evidence further supporting the association of ribosomes with the CPLs by demonstrating that the sedimentation properties of the small ribosomal subunit protein, S6, are dramatically altered in *Padi6*$^{-/-}$ oocytes. We also show that the abundance and localization of ribosomal components is dramatically affected in *Padi6*$^{-/-}$ two-cell embryos and that de novo protein synthesis is also dysregulated in these embryos. Finally, we demonstrate that embryonic genome activation (EGA) is defective in *Padi6*$^{-/-}$ two-cell embryos. These results suggest that, in mammals, ribosomal components are stored in the oocyte CPLs and are required for protein translation during early development.

KEY WORDS: Oocyte, Cytoplasmic lattice, Peptidyl arginine deiminase 6, Maternal effect gene, Ribosomal storage, Translational regulation, Embryonic genome activation, Ribosomal protein S6

INTRODUCTION

Eggs of most lower organisms contain an abundance of stored ribosomes that facilitate translation in the early embryo until the embryonic genome is activated (EGA) (Davidson, 1986). In *Xenopus* and *Drosophila*, while EGA occurs relatively quickly in real time (<10 hours) it does not initiate until after at least the 12th cell division. In mammals, however, while taking more than 2-4 days to occur, EGA actually initiates after just one cell division in the mouse and after two or three cell divisions in humans, cattle and sheep (Schultz, 2002). Given these observations, it has remained unclear as to whether mammalian oocytes need to maintain a storehouse of maternal ribosomes. Nevertheless, biochemical data in the mouse indicate that 75-80% of ribosomes are not incorporated into polysomes at ovulation and do not engage in protein synthesis in vitro (Bachvarova and De Leon, 1977).

Several lines of evidence suggest that these inactive ribosomes are actually embedded in the oocyte cytoplasmic lattices (CPLs), a fibrillar matrix composed of a proteinaceous component and RNA. Previous investigators have observed that a precursor-product relationship exists between ribosomes and the CPLs during oocyte growth, with the number of ribosomes decreasing as the density of CPLs increases (Garcia et al., 1979; Sternlicht and Schultz, 1981; Wassarman and Josefowicz, 1978). Furthermore, roughly two-thirds of the ribosomes predicted to exist, based on total rRNA levels, cannot be visualized at the ultrastructural level in fully grown oocytes (Garcia et al., 1979; Zamboni, 1970). The observation that the CPL fibrils contain repeating units of electron-dense ribosome-sized particles suggested that these 'missing' ribosomes are actually contained within the CPLs (Sternlicht and Schultz, 1981). Finally, unlike somatic cell ribosomes, which require centrifugal forces of at least 100,000 ***g*** (>1 hour) for pelleting, roughly 70% of oocyte rRNA partitions in the cell pellet following centrifugation at 9000 ***g*** (5 minutes), suggesting that most egg ribosomes are associated with a large supramolecular complex (Bachvarova et al., 1981). An additional series of experiments has suggested that the lattices also contain intermediate filaments such as keratin, leading to the hypothesis that they represent a unique oocyte cytoskeletal element (Capco et al., 1993; McGaughey and Capco, 1989). Given that many components of the protein synthetic machinery form associations with intermediate filaments, this interpretation does not diminish the possibility that the CPLs also contain ribosomes (Hesketh and Pryme, 1991; Hovland et al., 1996).

Most recently, our work has implicated peptidyl arginine deiminase 6 (PADI6), a highly abundant oocyte- and early embryo-restricted protein, in lattice regulation. In an initial study characterizing this novel oocyte factor, we showed by immuno-electron microscopy (immuno-EM) that PADI6 localizes primarily to the CPLs in mature oocytes (Wright et al., 2003). Then, in order to investigate PADI6 function, we inactivated the *Padi6* gene in mice and found that *Padi6*$^{-/-}$ females are infertile, with the developmental arrest occurring at the two-cell stage. This established *Padi6* as a novel mammalian maternal effect gene. Additionally, we found that the CPL structure cannot be visualized in *Padi6*$^{-/-}$ metaphase II-arrested oocytes, suggesting that PADI6 is required for CPL formation and/or maintenance and that the lattices are required for development beyond the two-cell stage (Esposito et

[1]Department of Genetic Medicine, Weill Medical College of Cornell University, 1300 York Avenue, New York, NY, USA. [2]Weill Graduate School of Medical Sciences of Cornell University, Weill Medical College of Cornell University, 1300 York Avenue, New York, NY, USA. [3]Department of Cell and Developmental Biology, Weill Medical College of Cornell University, 1300 York Avenue, New York, NY 10021, USA. [4]NV Organon, Oss, The Netherlands.

*These authors contributed equally to this work
†Present address: Baker Institute for Animal Health, College of Veterinary Medicine, Cornell University, Ithaca, NY 14850, USA
‡Author for correspondence (e-mail: sac269@cornell.edu)

Accepted 26 May 2008

al., 2007). This also established the *Padi6*$^{-/-}$ mouse as an ideal model system in which to test a number of the above hypotheses concerning lattice function.

Here, we present findings that further strengthen the model that the CPLs are involved in ribosomal storage in oocytes and that PADI6 is critical for lattice formation. We also show that, in *Padi6*$^{-/-}$ two-cell embryos, ribosomal component levels are reduced and de novo protein synthesis is dysregulated. Finally, we establish that the mechanism of the two-cell arrest in *Padi6*$^{-/-}$ embryos is probably due to a failure to completely activate the embryonic genome. Taken together, these findings underscore the potential importance of lattices in mammalian early development.

MATERIALS AND METHODS

Collection and preparation of oocytes and preimplantation embryos

The generation of the *Padi6*$^{-/-}$ mouse line is described by Esposito et al. (Esposito et al., 2007). All germinal vesicle (GV) stage oocytes and two-cell embryos were collected from 3- to 5-week-old *Padi6*$^{+/+}$ and *Padi6*$^{-/-}$ female mice. GV stage oocytes were isolated from ovarian follicles ~46 hours after PMSG (5 IU) stimulation and two-cell embryos were isolated from the oviducts of superovulated and mated female mice ~44 hours after hCG (5 IU) treatment.

Electron microscopy

For EM analysis of primordial follicle and growing oocytes, ovaries were collected from 14-day-old and 7-week-old females, respectively. They were fixed for 2 hours in 2.5% glutaraldehyde, 4% paraformaldehyde and 0.1% tannic acid in 0.1 M sodium cacodylate buffer (pH 7.3) (TA). GV oocytes and two-cell embryos were collected as described above, washed in PBS, pipetted onto polylysine-coated coverslips and fixed in TA for 2 hours. The cells were then incubated for 1 hour with 1% osmium tetroxide and stained with uranyl acetate en bloc. The eggs were then dehydrated through a series of graded ethanols and embedded in Spurr's resin (Electron Microscopy Sciences, Hatfield, PA). Semi-thin (0.5 μm), then ultra-thin (55-60 nm, silver-gold) sections were cut using a Diatome diamond knife on a Leica Ultracut S Ultramicrotome (Leica, Vienna, Austria), contrasted with lead citrate and viewed on a JEM 100 CX-II electron microscope (JEOL, USA, Peabody, MA) operated at 80 kV. Images were recorded on Kodak 4489 Electron Image film then digitized on an Epson Expression 1600 Pro scanner at 1200 dpi for publication. For electron microscopy analysis of the 9000 ***g*** pellet, 20 *Padi6*$^{+/+}$ and *Padi6*$^{-/-}$ GV stage oocytes were ruptured in 200 μl of rupture buffer and centrifuged as described below. The cell pellets were fixed in 2% glutaraldehyde in 0.05 M sorenson phosphate buffer and encapsulated in 1% agarose. Samples were then rinsed in buffer and post-fixed in 1% OsO_4. Next, the agarose pellets were released from centrifuge tubes, excess agarose was trimmed away, and the samples were processed as above.

Western blot and qRT-PCR analysis

For western blotting, *Padi6*$^{+/+}$ and *Padi6*$^{-/-}$ GV stage oocytes (30) and two-cell embryos (30) were isolated, boiled for 5 minutes in Laemmli buffer, and directly loaded onto a 10% SDS-PAGE gel. Proteins were separated at 200 V for 50 minutes and then transferred to a nitrocellulose membrane by applying current of 90 V for 90 minutes. All blots were blocked with 5% nonfat dry milk in TBS containing 0.5% Tween-20 (TBS-T), washed and incubated with a 1:1000 dilution of anti-ribosomal S6 sera (rabbit mAb, Cell Signaling, Danvers, MA) in 5% BSA or anti-tubulin sera (1:1000 dilution, Millipore, Temecula, CA) in blocking buffer overnight at 4°C. The blots were then washed three times for 10 minutes in TBS-T and incubated with 1:10,000 dilution of peroxidase-conjugated goat anti-rabbit IgG or donkey anti-mouse IgG secondary antibody (Jackson ImmunoResearch, West Grove, PA) for 1 hour. Following incubation in secondary antibody, the membranes were washed three times for 10 minutes in TBS-T, and Immobilon Western HRP Chemiluminescent Substrate (Millipore, Temecula, CA) was applied for 5 minutes and developed. The experiments were repeated three times.

For real-time RT-PCR quantitation of mRNAs, total RNA was isolated from 35 GV stage oocytes using Trizol and chloroform. The RNA contained within the aqueous fraction was then purified using RNeasy Mini Kit (Qiagen, Valencia, CA), reverse transcribed, and subjected to real-time PCR using sequence-specific 18S rRNA primers for TaqMan Gene Expression Assays (Applied Biosystems, Foster City, CA). PCR was performed using the TaqMan PCR Master Mix and the ABI 7700 thermal cycler (Applied Biosystems) using the following parameters: 50°C for 2 minutes and 95°C for 10 minutes, followed by 40 cycles at 95°C for 15 seconds and 60°C for 1 minute. 18S rRNA expression levels were normalized to Gapdh mRNA and quantitated using the $2^{-\Delta\Delta}$ CT method.

Oocyte fractionation and immuno slot-blot analysis

For sedimentation analysis, *Padi6*$^{+/+}$ and *Padi6*$^{-/-}$ GV oocytes were isolated from follicles and immediately ruptured in 200 μl of a buffer containing 0.05 M KCl, 0.2 M sucrose, 50 mM KCl, 0.5% Triton X-100, 10 mM HEPES (pH 7.3) and complete protease inhibitor cocktail (Roche, Branchburg, NJ, USA) using a ~60 μm (inner diameter) pulled Pasteur pipette. The lysate was then centrifuged at 650 ***g*** for 5 minutes at room temperature and the supernatant was centrifuged again at 9000 ***g*** for 5 minutes. The supernatant and pellet fractions were then incubated on ice in lysis buffer (50 mM Tris HCl, 150 mM NaCl, 1% NP40, and protease inhibitors) for 2 hours, heated to 100°C for 5 minutes in Laemmli buffer and directly loaded onto a PVDF membranes (Immobilon, Millipore, Billerica, MA) using a slot-blot apparatus (Hoefer, San Francisco, CA). The blots were then probed with anti-S6 and anti-PADI6 antibodies as described above.

Scanning confocal and wide-field microscopy, and immunofluorescence analysis

Following collection as described above, oocytes and embryos were either immediately fixed in 4% paraformaldehyde in Dulbecco's PBS (DPBS) (Invitrogen) for 30 minutes at room temperature or incubated first for 20 minutes in extraction buffer (0.1 M KCl, 20 mM $MgCl_2$, 3 mM EGTA, 20 mM HEPES (pH 6.8), 1% Triton X-100, Complete Protease Inhibitor Cocktail (Roche, Mannheim, Germany) then rinsed quickly three times in DPBS. The oocytes/embryos were then washed five times in IF buffer (DPBS, 1% BSA, 0.5% NGS), permeabilized with 0.5% Triton X-100 in PBS for 30 minutes, washed again (five times in IF), and incubated with guinea pig anti-PADI6 (1:500) (Wright et al., 2003), rabbit anti-S6 (1:200), rabbit anti-RNA Pol II (1:100, N-20, Santa Cruz Biotechnology), mouse anti-RNA Pol II CTD phospho-serine 2 (1:400, H5, Covance Research Products, Berkeley, CA), rabbit anti-spindlin (1:200, a generous gift from Barbara Knowles, The Jackson Laboratory, Bar Harbor Maine), rabbit anti-DNMT1 (1:400, PATH52 antiserum a generous gift from Timothy Bestor) or anti-H4K5 acetyl (1:200, Millipore, Billerica, MA) antibody in IF buffer overnight at 4°C. Oocytes/embryos were washed again (five times in IF) and incubated for 2 hours at room temperature with a 1:450 dilution of the appropriate secondary antibody: goat anti-guinea pig Alexa Fluor 546, goat anti-rabbit Alexa Fluor 488 or goat anti-mouse Alexa Fluor 633 (Molecular Probes, Eugene, OR). Oocytes and embryos were mounted on slides in Slowfade Gold antifade reagent (Molecular Probes, Eugene, OR), and imaged using an LSM 510 laser scanning confocal microscope (Zeiss). Extensive optimization was performed while imaging to ensure that we were as near to the theoretical resolution limit (~200 nm) as possible. Data were analyzed with MetaMorph 7 (Molecular Devices, Downingtown, PA) and colocalization analysis was performed using Volocity 4 (Improvision, Lexington, MA). Using MetaMorph7 for quantification of nuclear markers in Fig. 5A, a region of interest was defined using the DAPI signal as a marker for nuclear boundaries. Then the average intensity of the region for the different channels was logged to an Excel file where the data were averaged and statistics could be calculated. Once the average was calculated for each group [H4K5acetyl: average intensity 2286.3 (n=32) *Padi6*$^{+/+}$ versus 2058.5 (n=24) *Padi6*$^{-/-}$ t-test two-tailed P=0.023; phospho-pol II: average intensity 935.6 (n=16) *Padi6*$^{+/+}$ versus 626.8 (n=23) *Padi6*$^{-/-}$ t-test two-tailed P=0.006; pol II: average intensity 1572 (n=16) *Padi6*$^{+/+}$ versus 1272 (n=22) *Padi6*$^{-/-}$ t-test two-tailed P=0.003], an image most closely matching the average signal intensity was chosen as a 'representative' nucleus. For DNMT1 localization, oocytes were imaged at 1000× using a Zeiss Axiovert-200 fluorescence microscope.

Total protein synthesis and resolution of radiolabeled proteins

GV oocytes and two-cell embryos were radiolabeled for 2 hours in CZB medium containing 1 mCi/ml of [^{35}S]methionine (>1000 Ci/mMol; Perkin Elmer, Shelton, CT, USA). Following radiolabeling, the embryos were washed in αMEM/PVA, then in PBS/PVA and frozen in liquid nitrogen until use. Total protein was precipitated for 1 hour using 10% trichloroacetic acid (TCA) dissolved in 1 M NaOH and assayed by scintillation counting. To visualize de novo protein synthesis patterns, 20 GV oocytes and 20 two-cell embryos were resolved using 10% SDS-PAGE as previously described (Conover et al., 1991). After electrophoresis, the gel was dried and exposed overnight to a phosphor imager screen. The radiolabeled proteins were then visualized using a Typhoon Triad PhosphorImager.

Transcription requiring complex analysis

Two-cell embryos were collected at 43-46 hours post hCG injection and radiolabeled for 2 hours in CZB medium containing 1 mCi/ml of [^{35}S]methionine (>1000 Ci/mMol; Perkin Elmer, Shelton, CT, USA). Following radiolabeling, the embryos were washed in αMEM/PVA, treated for 10 minutes (room temperature) in a solution containing 50 mM Tris-HCl (pH 7.4), 2% Triton-X100 and 0.3 M KCl to enrich for the TRC proteins. Labeled proteins were then resolved by SDS-PAGE (10% gel) as described previously (Conover et al., 1991). The radiolabeled proteins were visualized using a Typhoon Triad PhosphorImager. TRC protein levels were quantified from tif files of the fluorograph by calculating the intensity of protein signal using the Photoshop Histogram Analysis program.

BrUTP incorporation assay

BrUTP incorporation assays were performed essentially as previously described (Aoki et al., 1997). Briefly, two-cell embryos were permeabilized for 2 minutes with 0.05% Triton X-100 in PB: 100 mM potassium acetate, 30 mM KCl, 1 mM $MgCl_2$, 10 mM Na_2HPO_4, 1 mM ATP, 1 mM DTT, supplemented with 1× complete protease inhibitor cocktail (Roche, Branchburg, NJ, USA) and 50 units/ml of RNasin. Treated embryos were then washed in PB and incubated for 10 minutes at 33°C in 100 mM potassium acetate, 30 mM KCl, 2 mM $MgCl_2$, 10 mM Na_2HPO_4, 2 mM ATP, 0.4 mM each of GTP, CTP and BrUTP. Next, embryos were washed in PB and the nuclear membrane was permeabilized in PB containing 0.2% Triton X-100 for 3 minutes. The embryos where washed again in PB and fixed with 4% paraformaldehyde for 30 minutes. BrUTP incorporation was detected by immunostaining using a 1:200 dilution of antiBrdU monoclonal antibody (Chemicon, Temecula, CA, USA). The embryos were then incubated with a 1:200 dilution of donkey anti-mouse FITC-labeled secondary antibody (Jackson ImmunoResearch) and processed as indicated in the immunofluorescence section. Following image capture, the signal was quantified from .tif files of the embryos using the Photoshop Histogram Analysis program by calculating the pixel value/unit area of five different random regions of the nucleus and five different region of the cytoplasm and by subtracting the average cytoplasmic value from the average nucleoplasm value. The transcription levels of the *Padi6*$^{-/-}$ nuclei were expressed as a percentage of the *Padi6*$^{+/+}$ transcription levels.

Statistical analysis

All experiments used for quantification were repeated at least three times. Statistical significance was assessed using the Microsoft Excel 2003 program using a two-tailed *t*-test.

RESULTS

PADI6 is required for cytoplasmic lattice formation in the growing oocyte

We used transmission electron microscopy (TEM) to investigate when the *Padi6*$^{-/-}$ defect first becomes evident during oogenesis and also to study the interrelationship of PADI6, CPLs and ribosomes in growing oocytes. Analysis of primordial follicle oocytes found no clear morphological differences between *Padi6*$^{+/+}$ oocytes (Fig. 1A) and *Padi6*$^{-/-}$ oocytes (Fig. 1B). This result was somewhat surprising, given that we have previously shown that the PADI6 protein is abundantly expressed at this developmental stage (Wright et al., 2003). Similar to previous reports (Zamboni, 1970), we next found that the CPLs first become evident in *Padi6*$^{+/+}$ oocytes at approximately the 40 μm stage of growth and appear to be derived from curvilinear 'intermediate structures' (IS), which have properties of both aggregated ribosomes (Rb) and mature lattices (Fig. 1C). However, no CPLs or IS were observed in ~40 μm *Padi6*$^{-/-}$ oocytes (Fig. 1D). CPLs were also evident in fully grown germinal vesicle (GV) stage *Padi6*$^{+/+}$ oocytes (Fig. 1E), whereas CPLs were not observed in similarly staged *Padi6*$^{-/-}$ oocytes (Fig. 1F). Non-lattice-associated ribosome levels appeared similar between stage-matched *Padi6*$^{+/+}$ and *Padi6*$^{-/-}$ oocytes. We found that CPLs were also not observed in *Padi6*$^{-/-}$ two-cell embryos (Fig. 1H) whereas lattices in *Padi6*$^{+/+}$ two-cell embryos were visible (arrows, Fig. 1G). As lattice structures are never detected at any stage of oocyte growth in *Padi6*$^{-/-}$ oocytes, we conclude that PADI6 is indeed required for lattice formation.

Overall levels of ribosomal components are not altered in *Padi6*$^{-/-}$ oocytes

To further evaluate the relationship between PADI6 and ribosomes, we next investigated whether total ribosome levels were altered in *Padi6*$^{-/-}$ oocytes. Analysis of 40S ribosomal subunit levels by quantitative real time(q) RT-PCR using 18S rRNA probes and by immunoblot analysis using an antibody reactive with the small ribosomal subunit protein, S6, found that loss of PADI6 does not affect levels of these ribosomal components (Fig. 2A). Therefore, lack of lattice formation does not appear to have consequences on overall ribosomal levels in the oocyte.

Ribosomal components display increased solubility in *Padi6*$^{-/-}$ oocytes

Given previous observations that 70% of oocyte rRNA can be pelleted at low centrifugal force (9000 ***g***), and therefore is most likely associated with a large supramolecular complex, we next wanted to test whether the majority of ribosomal S6 protein also pellets at 9000 ***g***. Furthermore, we reasoned that if the lattices are indeed the supramolecular complex associated with stored ribosomal components, S6 should pellet less readily in *Padi6*$^{-/-}$ oocytes. Accordingly, we ruptured *Padi6*$^{+/+}$ and *Padi6*$^{-/-}$ oocytes in a hypotonic 0.05 M KCl buffer containing 0.2 M sucrose and 0.5% Triton X-100, and serially centrifuged the oocyte lysates for 5 minutes at 650 and 9000 ***g***. Ribosomal protein levels were then evaluated by immuno-slot-blot analysis using the S6 antibody. Results show that the majority of the S6 protein partitioned in either the 650 or 9000 ***g*** pellet in *Padi6*$^{+/+}$ oocytes (Fig. 2B). This finding further supports the hypothesis that, in mammalian oocytes, ribosomal components are associated with a supramolecular complex. In *Padi6*$^{-/-}$ oocytes, however, most of the S6 protein partitioned in the supernatant fraction following rupture and centrifugation (Fig. 2B). We next performed TEM analysis of the *Padi6*$^{+/+}$ and *Padi6*$^{-/-}$ 9000 ***g*** oocyte lysate pellets to test the hypothesis that the CPLs represent this complex. Results show that the major distinction between these two samples was that, although an abundance of lattice-like structures were found in the *Padi6*$^{+/+}$ oocyte pellet (arrow, Fig. 2C), these structures were not observed in the *Padi6*$^{-/-}$ oocyte pellet (Fig. 2D). Interestingly, ribosomes appear to be directly associated with some of the putative CPL structures (arrowheads). In further support of the hypothesis that ribosomes are contained within CPLs, we also found by immuno-slot-blot analysis that PADI6, which localizes to CPLs, mainly partitions in the 9000 ***g*** pellet of *Padi6*$^{+/+}$ oocyte lysates (data not shown). Taken together,

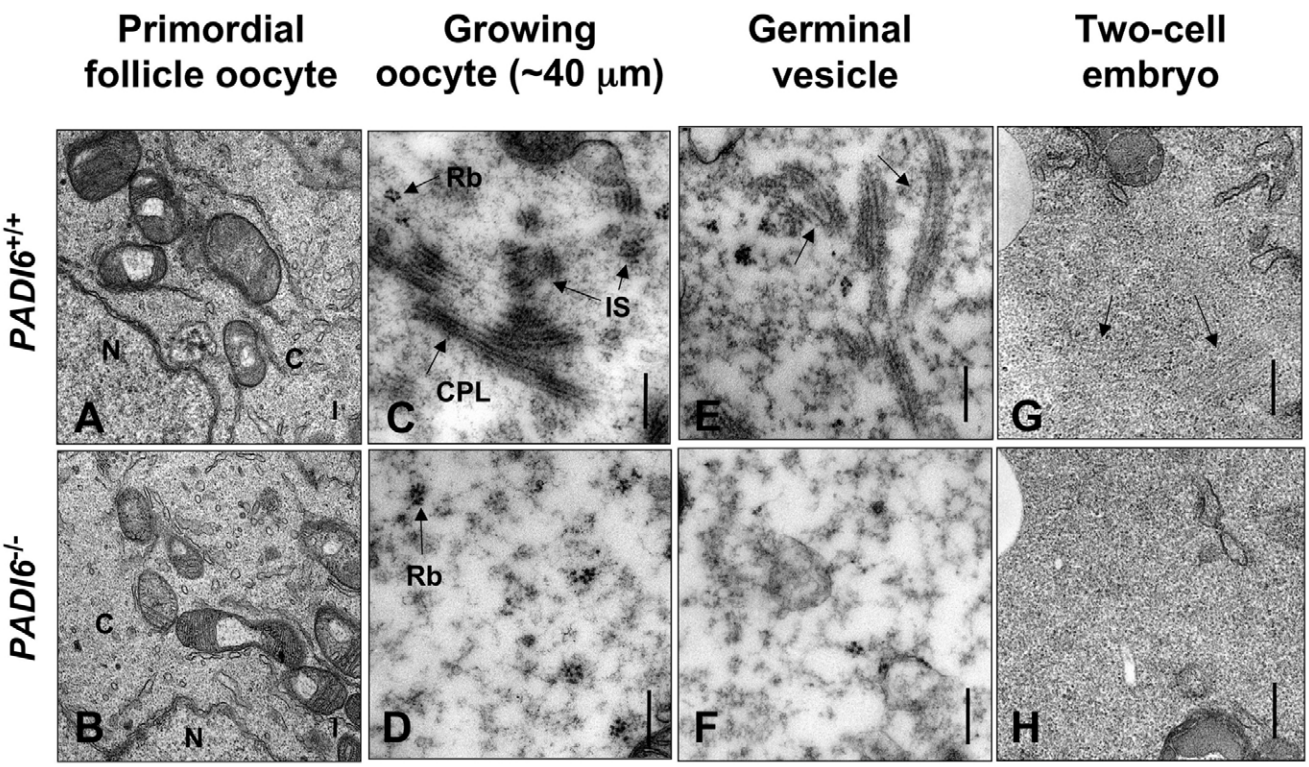

Fig. 1. PADI6 is required for cytoplasmic lattice formation in oocytes and two-cell embryos. (**A**) *Padi6*$^{+/+}$ primordial follicle oocyte. N, nucleus; C, cytoplasm. (**B**) *Padi6*$^{-/-}$ primordial follicle oocyte. (**C**) CPLs are first observed in *Padi6*$^{+/+}$ growing oocytes. Rb, ribosome; IS, intermediate structure; CPL, cytoplasmic lattice. (**D**) CPLs do not form in *Padi6*$^{-/-}$ growing oocytes. (**E**) CPLs are also observed in *Padi6*$^{+/+}$ fully grown germinal vesicle stage oocytes. (**F**) CPLs are not observed in *Padi6*$^{-/-}$ fully grown germinal vesicle stage oocytes. (**G**) Arrows highlight CPLs in *Padi6*$^{+/+}$ two-cell embryos. (**H**) CPLs are not observed in *Padi6*$^{-/-}$ two-cell embryos. Scale bar: 200 nm. These experiments were repeated twice.

the above findings support the hypothesis that the CPLs contain ribosomal components and that PADI6 is required for their incorporation.

PADI6 and S6 appear to colocalize in oocytes and S6 localization is disrupted in *Padi6*$^{-/-}$ oocytes

We further tested the hypothesis that the CPLs contain ribosomal components using laser scanning confocal microscopy and immunofluorescence analysis to determine whether PADI6 and S6 colocalize in *Padi6*$^{+/+}$ oocytes, and also whether S6 localization is altered in *Padi6*$^{-/-}$ oocytes, as would be expected in the absence of CPLs. Owing to the high abundance and diffuse staining pattern of PADI6 and S6 in GV oocytes, our initial colocalization analysis was not reliable. It has previously been demonstrated that the CPLs are detergent insoluble following 1% Triton X-100 (Triton) extraction (Capco et al., 1993; McGaughey and Capco, 1989), and we found that Triton extraction before fixation allowed us to test more reliably for colocalization. Similar techniques are used for visualization of proteins associated with the cytoskeleton (Spector, 1998). Results show that, in Triton extracted oocytes, PADI6 and S6 appear to colocalize in regions throughout the cytoplasm and at granular foci in the oocyte cortex (Fig. 3A). We further controlled for random colocalization owing to high abundance of both factors by observing the extent of colocalization before and after a 20 pixel shift of one of the channels with respect to the other. Random colocalization should not be dramatically affected by a pixel shift. We observed a reproducible reduction in colocalization by 30% after the pixel shift, therefore, at least 30% of our observed colocalization is not due to random overlap. Given that the theoretical resolution limit of our confocal analysis (~200 nm) is larger than the repeating units of the lattices (~21nm), we next attempted to localize the S6 ribosomal protein to the lattices by immuno-EM. Unfortunately, however, we were not able to obtain specific labeling of oocytes using either the S6 antibody or other commercially available ribosomal protein antibodies. Thus, we proceeded with our confocal analysis, as it was the highest resolution method available.

Confocal analysis further revealed that S6 is retained in the insoluble fraction in Triton extracted *Padi6*$^{-/-}$ oocytes; however, the staining is more punctate than in extracted *Padi6*$^{+/+}$ oocytes. Most striking, however, is the complete absence of S6 from the cortex of *Padi6*$^{-/-}$ oocytes (arrow, Fig. 3A). It has been observed that a number of other proteins, including actin (Sun and Schatten, 2006) and DNMT1 (Ratnam et al., 2002), also abundantly localize to the oocyte cortex. To test whether the localization of these factors is also affected by loss of PADI6, we first probed intact oocytes with an antibody specific for DNMT1. We found by wide-field immunofluorescence microscopy that DNMT1 localization does not appear to be affected in *Padi6*$^{-/-}$ oocytes (Fig. 3C). Because actin is Triton insoluble, we then probed Triton-extracted oocytes with phalloidin and found that the actin network in the cortex is intact in *Padi6*$^{-/-}$ oocytes (Fig. 3B). Therefore, we predict that PADI6 and/or the CPLs are responsible for the specific targeting of ribosomal components to the oocyte cortex, and that, in their absence, proper

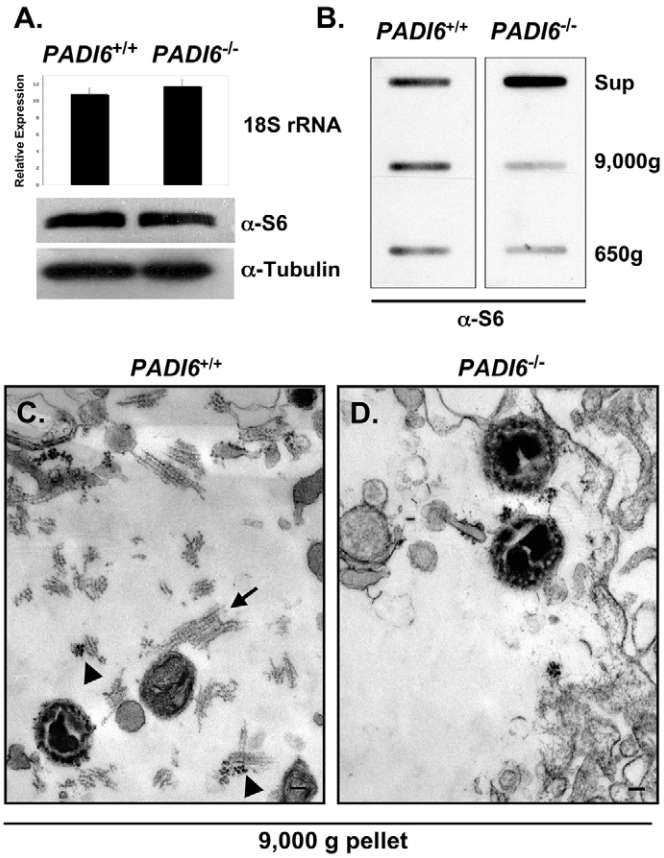

Fig. 2. Ribosomal components display increased solubility in *Padi6*$^{-/-}$ oocytes. (**A**) qRT-PCR analysis using 18S rRNA primers and western blot analysis using anti-S6 antibodies indicates that levels of ribosomal components are similar between *Padi6*$^{+/+}$ and *Padi6*$^{-/-}$ oocytes. (**B**) In contrast with *Padi6*$^{+/+}$ oocytes, the majority of ribosomal protein S6 partitions in the supernatant of ruptured *Padi6*$^{-/-}$ oocytes. Oocytes were ruptured in hypotonic buffer, serially centrifuged at 650 and 9000 ***g*** for 5 minutes, and the partitioning of ribosomal components into the supernatant (Sup) and pellet fractions was evaluated by immuno-slot-blot analysis using anti-S6 antibodies. (**C**) Transmission electron microscopic analysis indicates that although putative CPLs (arrow) are observed in the *Padi6*$^{+/+}$ 9000 ***g*** oocyte pellet, (**D**) lattices are not observed in the *Padi6*$^{-/-}$ oocyte pellet. Arrowheads highlight ribosome-like particles associated with CPLs. Scale bar:100 nm. Values for the qRT-PCR are represented as the mean±s.e.m. from three independent experiments (P=0.407). The immunoblotting experiments were repeated three times and the electron microscopy experiments were repeated twice.

targeting does not occur. Taken together, these results further strengthen the interrelationship between PADI6, ribosomal components and the CPLs.

De novo protein synthesis is not globally altered in *Padi6*$^{-/-}$ oocytes

Given several lines of evidence that lattices are involved in maternal ribosome storage and our observation that lattices do not form in *Padi6*$^{-/-}$ oocytes and early embryos, these cells represent a unique model system in which to study the function of stored ribosomes during oogenesis and early development. Although previous investigators predicted that the stored ribosomes are involved in translation following fertilization (Bachvarova et al., 1981), it is also possible that these ribosomes play a role in protein synthesis in oocytes. To test this hypothesis, we metabolically labeled *Padi6*$^{+/+}$ and *Padi6*$^{-/-}$ GV stage oocytes for 2 hours using [^{35}S]methionine and evaluated de novo protein synthesis by scintillation counting and fluorography of resolved proteins. Results showed that there were no reliable differences in overall translation levels (data not shown) and, with few exceptions, the repertoire of nascently synthesized proteins appears similar between *Padi6*$^{+/+}$ and *Padi6*$^{-/-}$ oocytes (Fig. 3D). The 72 kDa protein (arrow) missing from *Padi6*$^{-/-}$ oocytes is probably PADI6. This result, coupled with the observation that oocyte growth and fertilization are not affected by loss of PADI6, supports the hypothesis that putative CPL-associated ribosomal components do not play a crucial role in protein translation in oocytes.

S6 protein levels are lower and localization is dramatically altered in *Padi6*$^{-/-}$ two cell embryos

Our previous finding that *Padi6*$^{-/-}$ embryos arrest at the two-cell stage suggested that putative CPL-associated ribosomal components are probably required for protein synthesis in the early embryo. To begin testing this hypothesis, we next evaluated S6 levels and localization by western blot and confocal immunofluorescence analysis in *Padi6*$^{+/+}$ and *Padi6*$^{-/-}$ two-cell embryos. Results show that both PADI6 and S6 strongly colocalize at the non-apposed cortical regions of each blastomere in *Padi6*$^{+/+}$ embryos (Fig. 4A). In *Padi6*$^{-/-}$ two-cell embryos, we found that total levels of S6 were reduced (Fig. 4A,D) and that S6 is not enriched at embryonic cortex. These observations suggest that, in contrast to the oocyte, PADI6 appears to be crucial for helping maintain proper ribosomal levels in the two-cell embryo. Furthermore, similar to our finding in oocytes, these observations suggest that PADI6 also appears to be required for localization of S6 to the embryonic cortex (arrows, Fig. 4C). The microfilament network is intact throughout the entire cortex region of blastomeres in both *Padi6*$^{+/+}$ and *Padi6*$^{-/-}$ two-cell embryos (Fig. 4B), indicating that PADI6 only appears to be required for targeting a specific subset of molecules to the embryonic cortex.

De novo protein synthesis is altered in *Padi6*$^{-/-}$ two cell embryos

To test the hypothesis that reduced levels and disrupted localization of S6 in *Padi6*$^{-/-}$ two-cell embryos affects protein translation, we next metabolically labeled the embryos with [^{35}S]methionine for 2 hours and then evaluated de novo protein synthesis by scintillation counting and by fluorography of resolved proteins. Results show that total protein synthesis levels were reduced by ~50% in *Padi6*$^{-/-}$ two-cell embryos compared with *Padi6*$^{+/+}$ embryos (data not shown). In addition to reduced global levels of protein synthesis, fluorographic analysis of newly synthesized proteins found that expression levels of specific proteins in *Padi6*$^{-/-}$ two-cell embryos are altered when compared with *Padi6*$^{+/+}$ embryos (Fig. 4E). In particular, synthesis of one protein at ~30 kDa is dramatically upregulated in the *Padi6*$^{-/-}$ two-cell embryo. Based on previous reports, we hypothesized that this protein was probably spindlin, the product of a stored maternal transcript thought to be involved in regulating the cell cycle during meiosis and the first mitotic cell division (Oh et al., 1997). We next tested the hypothesis that spindlin protein synthesis is dysregulated in *Padi6*$^{-/-}$ two-cell embryos by confocal analysis using anti-spindlin antisera and found that spindlin levels were, in fact, increased in *Padi6*$^{-/-}$ two-cell embryos (Fig. 4F). It is currently unclear why, in addition to the observed increase in cytoplasmic spindlin levels in *Padi6*$^{-/-}$ two-cell embryos, levels of spindlin also appear to be increased in the perivitelline space of these embryos; however, this may be due to leakage of the protein during fixation.

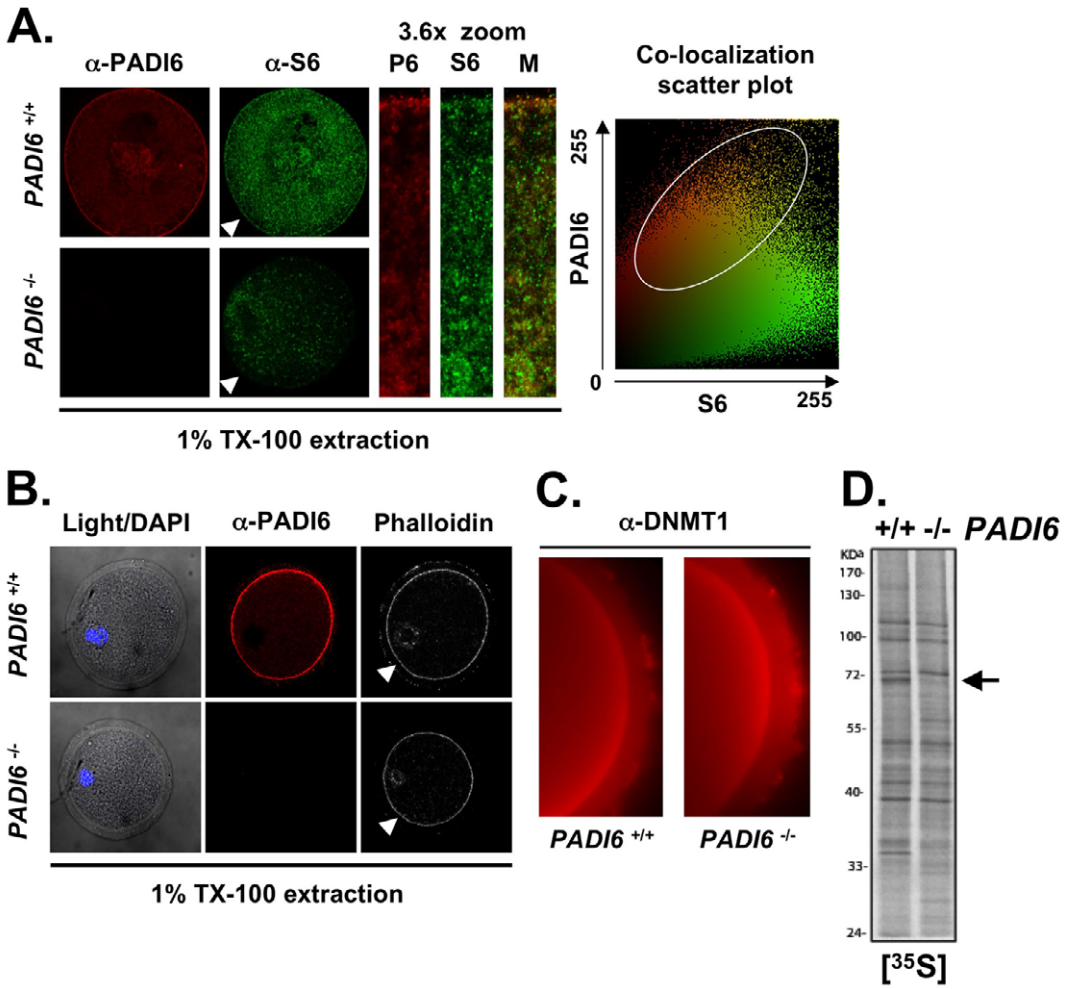

Fig. 3. PADI6 and ribosomal protein S6 colocalize in Triton X-100 extracted oocytes and loss of PADI6 alters S6 localization but not de novo protein synthesis. (**A**) PADI6 (P6) colocalizes with ribosomal protein S6 in Triton X-100 extracted GV stage *Padi6*$^{+/+}$ oocytes and S6 localization is altered in *Padi6*$^{-/-}$ oocytes. PADI6 and S6 co-localization in *Padi6*$^{+/+}$ oocytes is highlighted in merged image (M). The degree of co-localization (oval) is shown in the scatter plot. S6 localization to the oocyte cortex (or lack thereof in the *Padi6*$^{-/-}$ oocytes) is highlighted by the arrowheads. (**B**) Phalloidin staining of Triton X-100 extracted GV oocytes reveals that the cortical actin network is not disrupted in *Padi6*$^{-/-}$ oocytes. (**C**) Wide-field immunofluorescence analysis shows that DNMT1 displays similar cortical localization in *Padi6* $^{+/+}$ and *Padi6*$^{-/-}$ GV stage oocytes. (**D**) Fluorographic analysis of [^{35}S]methionine labeled proteins from *Padi6*$^{+/+}$ and *Padi6*$^{-/-}$ GV stage oocytes. Arrow indicates a protein that, based on its molecular weight (~72 kDa) and absence from *Padi6*$^{-/-}$oocytes, is probably PADI6. These experiments were repeated three times.

Taken together, these observations support the hypothesis that improper CPL formation in *Padi6*$^{-/-}$ oocytes leads to an overall reduction in protein synthesis in two-cell embryos. Furthermore, the altered translation pattern in *Padi6*$^{-/-}$ two-cell embryos suggests that the CPL complex may also play a role in organizing and regulating the translational machinery such that specific maternal mRNAs are translated at different efficiencies in *Padi6*$^{-/-}$ embryos compared with *Padi6*$^{+/+}$ embryos. The observation that spindlin levels are increased in *Padi6*$^{-/-}$ embryos also suggests that the observed overall reduction in total protein synthesis is not simply due to cell death.

Embryonic genome activation is incomplete in *Padi6*$^{-/-}$ embryos

Previous investigators have shown that protein synthesis is required for major genome activation at the two-cell stage in mice (Wang and Latham, 1997). Therefore, we next tested the hypothesis that the observed translational defects in *Padi6*$^{-/-}$ two-cell embryos lead to defective EGA. In mammals, nuclear translocation of maternally inherited RNA Polymerase II (RNA Pol II) is thought to be a major determinant of EGA (Bellier et al., 1997). Therefore, we first investigated whether RNA Pol II levels and/or localization was specifically affected by loss of PADI6. We probed two-cell embryos with an antibody that recognizes the N terminus of RNA Pol II and found that levels of RNA Pol II were reduced by ~20% in the nucleus of *Padi6*$^{-/-}$ two-cell embryos when compared with *Padi6*$^{+/+}$ embryos (Fig. 5A). Furthermore, we also found that levels of phosphorylated (Ser 2) RNA Pol II (a well characterized marker for active transcription) (Palancade and Bensaude, 2003) were reduced by ~30% in the nucleus of *Padi6*$^{-/-}$ embryos (Fig. 5A). These results suggest that both RNA Pol II nuclear translocation and RNA Pol II-mediated transcription are reduced in *Padi6*$^{-/-}$ embryos. In addition, our metabolic labeling data suggests that the basis for the nuclear translocation deficiency may lie in the improper translation of factors required for the transport of RNA Pol II from the cytoplasm

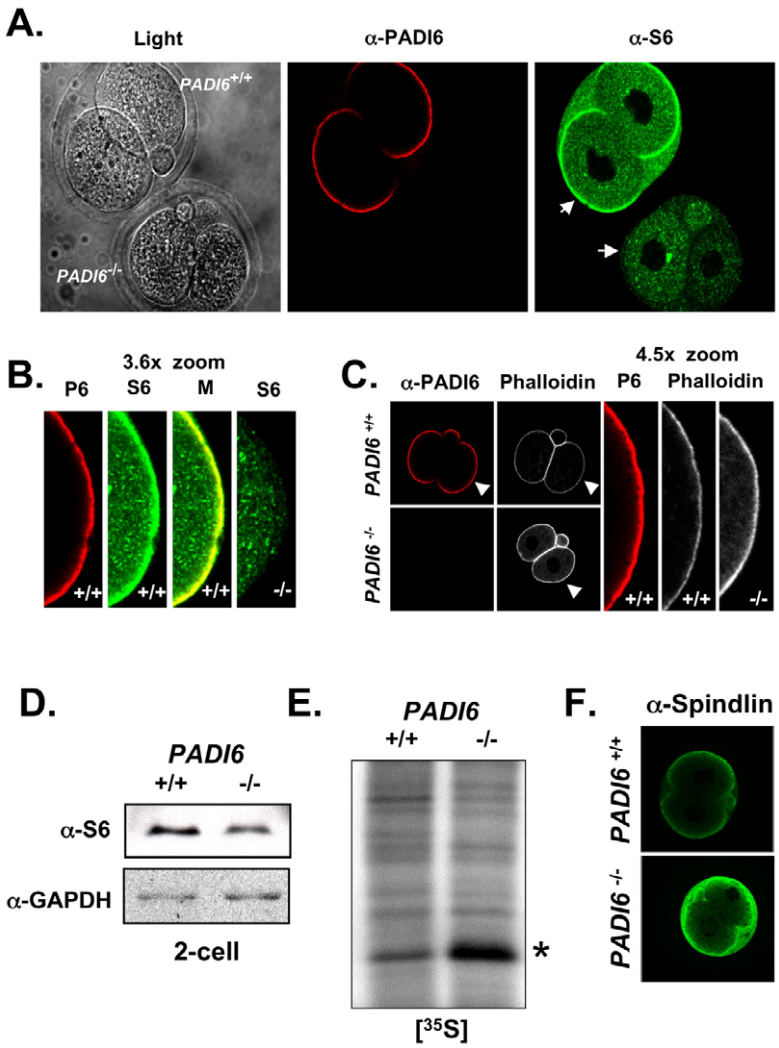

Fig. 4. Loss of PADI6 alters the levels and localization of ribosomal protein S6 and affects protein synthesis in two-cell embryos. (**A**) PADI6 (P6) colocalizes with S6 at the non-apposed cortical regions of *Padi6*$^{+/+}$two-cell embryo blastomeres, whereas S6 is absent from the embryonic cortex in *Padi6*$^{-/-}$ two-cell embryos (arrows and **B**). (**C**) Phalloidin staining reveals that the cortical actin network is not disrupted in *Padi6*$^{-/-}$ two cell embryos. (**D**) Western blot analysis of protein extracts indicates that S6 levels are reduced in *Padi6*$^{-/-}$ two-cell embryos. (**E**) Fluorographic analysis of [^{35}S]methionine labeled proteins indicates that specific mRNAs are translated at different efficiencies in *Padi6*$^{-/-}$ two-cell embryos. Asterisk indicates putative spindlin protein. (**F**) Confocal immunofluorescence analysis confirms that spindlin expression is upregulated in *Padi6*$^{-/-}$ two-cell embryos. These experiments were repeated three times.

to the nucleus. This hypothesis is supported by the observation that RNA Pol II appears to aggregate outside of the nuclear envelope in *Padi6*$^{-/-}$ embryos (Fig. 5A). Given that histone H4 acetylation is well correlated with active gene transcription (Roth et al., 2001), we next probed *Padi6*$^{+/+}$ and *Padi6*$^{-/-}$ two-cell embryos with an anti-histone H4 acetyl antibody (histone H4K5) as a further test of the effects of loss of PADI6 on embryonic transcription. Results show a small, but statistically significant, ~10% reduction in histone H4 acetylation in *Padi6*$^{-/-}$ two-cell embryo nuclei when compared with *Padi6*$^{+/+}$ embryos (Fig. 5A). We next measured nuclear incorporation of BrUTP in *Padi6*$^{+/+}$ and *Padi6*$^{-/-}$ two-cell embryos using an anti-BrUTP antibody and fluorescence microscopy (Aoki et al., 1997). Fluorescence analysis showed that transcription levels were reduced by ~73.7% in *Padi6*$^{-/-}$ embryos compared with *Padi6*$^{+/+}$ embryos (Fig. 5B). Finally, we investigated the de novo synthesis of the transcription requiring complex (TRC), a group of Triton X-100 insoluble proteins that are the first major products of embryonic transcription and thus function as a marker for EGA (Schultz et al., 1999). Results show that TRC synthesis is reduced by ~53% in *Padi6*$^{-/-}$ two-cell embryos when compared with *Padi6*$^{+/+}$ embryos (Fig. 5C), thus further supporting the hypothesis that *Padi6*$^{-/-}$ two-cell embryos fail to undergo complete embryonic genome activation. Interestingly, others have noted that inhibiting embryonic transcription (as evaluated by TRC synthesis) also inhibits the development-associated decrease in spindlin synthesis (Worrad et al., 1995); thus, our observation of the inverse relationship between embryonic transcription and spindlin synthesis is in line with previous findings.

DISCUSSION

In this report, we take advantage of the unique absence of cytoplasmic lattices in *Padi6*$^{-/-}$ mouse oocytes to revisit and strengthen a long-standing hypothesis that the lattices are a storage structure for maternal ribosomes. We also further characterize defects in these oocytes and embryos to better understand the significance of the loss of PADI6 and/or the lattices at different stages of development.

Our findings support the hypothesis that improper CPL formation *Padi6*$^{-/-}$ oocytes affects ribosomal storage leading to overall lower levels of de novo protein synthesis in the two-cell embryo and to dysregulation of the translational program. Furthermore, we predict that this change in protein synthesis leads to incomplete activation of the embryonic genome and, subsequently, arrest at the two-cell stage. Our results also demonstrate that the mechanism of the *Padi6*$^{-/-}$ two-cell arrest actually initiates during oocyte growth. Previously, we reported an absence of lattices in ovulated mature *Padi6*$^{-/-}$ oocytes (Esposito et al., 2007). However, considering the number of dramatic ultrastructural rearrangements that occur

between oocyte growth and maturation, it was possible that PADI6 was necessary for lattice maintenance and not formation. Here, we undertook a more comprehensive ultrastructural study of lattice formation from the primordial oocyte stage until the two-cell embryo. In agreement with previous studies, we found in *Padi6*$^{+/+}$ oocytes that the lattices first become apparent in the growing oocyte. Additionally, we were able to detect all of the putative steps of lattice formation from aggregated polysomes and curvilinear intermediate structures to elongated linear lattices. In striking contrast, however, we never observed any stages of lattice formation in any *Padi6*$^{-/-}$ oocytes. Thus, we conclude that PADI6 is necessary for the earliest stages of lattice formation.

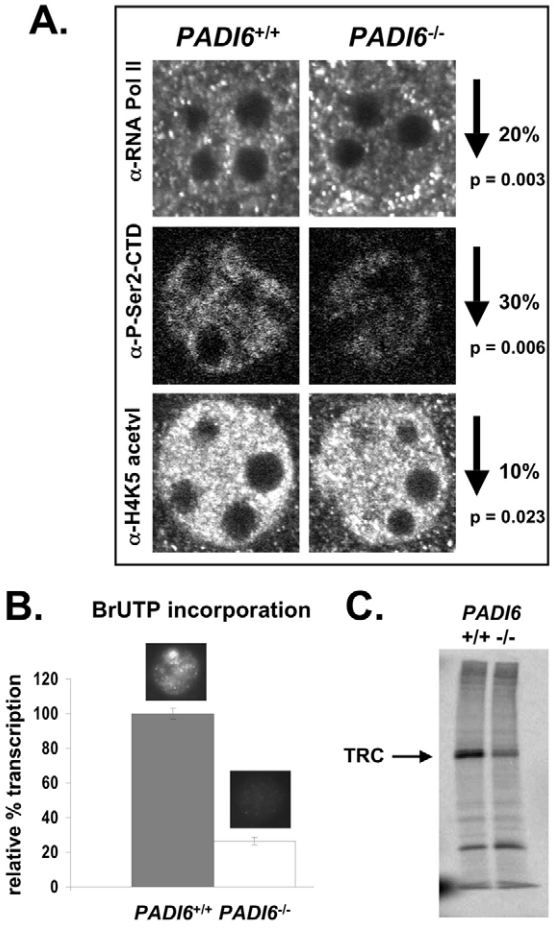

Fig. 5. Embryonic genome activation is defective in *Padi6*$^{-/-}$ two-cell embryos. (**A**) Levels of RNA polymerase II (RNA Pol II), phosphorylated RNA Pol II (P-Ser2-CTD) and acetylated histone H4 (H4K5 acetyl) are significantly reduced in *Padi6*$^{-/-}$ two-cell embryos. Representative nuclei shown were chosen based on their average signal intensity matching the respective mean of average intensities for *Padi6*$^{+/+}$ and *Padi6*$^{-/-}$ embryo nuclei. Values represent the mean signal intensity±s.e.m. (**B**) BrUTP incorporation into the nucleus of *Padi6*$^{-/-}$ two-cell embryos is significantly reduced. Representative nuclei are shown above bars in histogram. Values represent the mean BrUTP nuclear incorporation±s.e.m. from three independent experiments (P<0.05). (**C**) Fluorographic analysis of [^{35}S]methionine labeled and Triton X-100 extracted two-cell embryos indicates that synthesis of transcription requiring complex (TRC) proteins is reduced in *Padi6*$^{-/-}$ embryos. These experiments were repeated three times.

Our ultrastructural investigation of two-cell embryos revealed that lattices, although present in *Padi6*$^{+/+}$ embryos, are still not detected in *Padi6*$^{-/-}$ embryos. Thus, we conclude that if the lattices cannot form during oocyte growth, they do not form after fertilization. This observation is consistent with the lattices being an oocyte storage structure from which maternal factors are released during early embryogenesis. Notably, other than the prominent lack of CPLs, the *Padi6*$^{-/-}$ embryos look surprisingly similar to the *Padi6*$^{+/+}$ embryos at the ultrastructural level. This further supports the model that it is indeed the absence of the lattices, and not another defect that ultimately results in the developmental arrest. This, taken together with our result that EGA is not complete in these arrested embryos, further strengthens the link between the lattices and proper early embryonic gene expression. It also argues against cell death being the mechanism of incomplete EGA in *Padi6*$^{-/-}$ embryos.

Previous reports found that, unlike in somatic cells, the majority of rRNA in murine oocyte is pelleted at low centrifugal forces (9000 ***g***). This finding lead to the conclusion that oocyte ribosomes are associated with a large supramolecular complex, most probably the lattices (Bachvarova et al., 1981; Brower and Schultz, 1982). In our current study, we strengthened the validity these reports of by showing that the ribosomal S6 protein readily pellets at 9000 ***g*** in *Padi6*$^{+/+}$ oocytes. If the CPLs were indeed the supramolecular structure with which the ribosomal components are associated, then one would expect the S6 protein to not pellet as readily in the *Padi6*$^{-/-}$ oocytes. This is indeed what we observed. Furthermore, our EM results showed that the major difference between the 9000 ***g*** pellets of *Padi6*$^{+/+}$ and *Padi6*$^{-/-}$ oocytes is the presence or absence of the lattices, respectively. Thus, we concluded that ribosomal components are probably associated with the lattices, and PADI6 is required for their incorporation. Our immunofluorescence analysis further strengthens this hypothesis. Probing Triton-extracted oocytes with antibodies specific for S6 and PADI6, we were able to demonstrate considerable colocalization.

Our immunofluorescence data also shows that, at the two-cell stage, PADI6 and S6 abundantly localize to the microfilament-rich embryo cortex. Our original immuno-EM data localizing PADI6 to the lattices was carried out in oocytes, so it is possible that, at the two-cell stage, PADI6 is targeted from the lattices to the microfilament network in the embryo cortex. Interestingly, in the absence of PADI6, S6 localization to the cortex is completely disrupted. This observation suggests that PADI6 may also play an important role in the proper localization of translational machinery in the early embryo.

Our [^{35}S]methionine labeling experiments show that protein translation is reduced in *Padi6*$^{-/-}$ embryos. Furthermore, we also found that the relative translation efficiency of specific embryonic transcripts is altered. The most dramatic example is spindlin, which is synthesized at relatively much higher levels in *Padi6*$^{-/-}$ embryos. Spindlin has previously been characterized in mammalian oocytes as a stored maternal transcript (Oh et al., 2000). This observation supports a model in which the lattices play a role not only in post-fertilization ribosome stability but also in translational control of certain stored maternal transcripts. Additionally, our observation of an overall reduction in protein synthesis in *Padi6*$^{-/-}$ embryos implies that failing to regulate maternal ribosomes properly does not directly lead to a global upregulation of all stored maternal messages. This would not be surprising, given the highly regulated nature of maternal mRNP complexes. Given that *Padi6*$^{-/-}$ embryos arrest at the two-cell stage and that EGA is incomplete in *Padi6*$^{-/-}$ embryos, we predict that some the affected maternal transcripts encode key reprogramming

factors. In our study, we observed that although abundant in the cytoplasm, RNA Pol II seems to aggregate in foci surrounding the nuclear envelope in *Padi6*$^{-/-}$ embryos. Thus, it is possible that one of the CPL-associated transcripts encodes a factor(s) that is/are responsible for targeting RNA Pol II to the nucleus. In addition, given that both S6 and PADI6 localize to, and become enriched in, the cortex of two-cell embryos, and that this enrichment is absent in *Padi6*$^{-/-}$ embryos, the cortex may represent a special organizing site for translation of maternal transcripts.

It is known that a significant fraction of the RNA synthesized during EGA is ribosomal RNA. As our characterizations show, a number of markers of active mRNA transcription are reduced by 10 to 30% in *Padi6*$^{-/-}$ embryos. Overall RNA synthesis, however, assayed by comparing BrUTP incorporation levels, is down by almost 75% in *Padi6*$^{-/-}$ embryos. Therefore, an alternative interpretation of the lower S6 levels in the two-cell *Padi6*$^{-/-}$ embryos is that nascent ribosomes are not being properly synthesized. The dramatically lower level of RNA synthesis, therefore, probably includes rRNAs, tRNAs, and non-coding regulatory RNAs in addition to mRNAs.

The mechanism of EGA in mammals is still not well understood. Our finding that the *Padi6*$^{-/-}$ developmental arrest occurs at the two-cell stage adds *Padi6* to a short list of known mammalian maternal effect genes. Interestingly, loss of most of the other known maternal effect genes such as MATER, Zar1, NPM2, Bnc1, Hsf1 and BRG1 also results in embryonic arrest around the two-cell stage of development (Bultman et al., 2006; Burns et al., 2003; Christians et al., 2000; Ma et al., 2006; Tong et al., 2004; Wu et al., 2003). EGA defects (as determined by measuring TRC levels) have been shown to underlie the developmental arrest phenotype of many of these maternal effect gene mutants; however, the detailed mechanisms leading to the EGA defect in these animals remain to be elucidated. Our finding that TRC levels are reduced by more than 50% in *Padi6*$^{-/-}$ embryos, suggests that EGA failure also underlies the *Padi6*$^{-/-}$ developmental arrest.

In summary, in this report we provide the first mechanistic study elucidating how a mammalian maternal effect gene such as PADI6 mediates activation of the embryonic genome. We take advantage of the absence of cytoplasmic lattices in *Padi6*$^{-/-}$ oocytes and embryos to first strengthen the model that the lattices represent a storage structure for maternal ribosomes. Furthermore, we also show that the levels and localization of ribosomal components are affected in *Padi6*$^{-/-}$ two-cell embryos, as is de novo protein synthesis. Additionally, we find that the relative expression levels of specific transcripts, including a well-characterized stored maternal transcript, are also altered in these embryos. These findings lead to the prediction that improper storage of ribosomal components in *Padi6*$^{-/-}$ oocytes during oocyte growth, leads to decreased levels of ribosomes and to a dysregulated translational program in *Padi6*$^{-/-}$ two-cell embryos. Furthermore, we predict that the altered protein synthesis pattern in *Padi6*$^{-/-}$ two-cell embryos then leads to a dramatic reduction in embryonic transcriptional activity and ultimately to embryonic arrest. Alternatively, however, it is possible that the lattices do not play a direct role in early developmental events and that PADI6 alone required for EGA and development beyond the two-cell stage. Studies to uncouple the relative contributions of lattice versus PADI6 loss to the *Padi6*$^{-/-}$ two-cell arrest are ongoing.

We are grateful to Roger Gosden, Rosemary Bachvarova and Elizabeth Lacy for their technical advice and critical reading of this manuscript. We thank Dr Barbara Knowles for the anti-spindlin antibody and Dr Timothy Bestor for the anti-DNMT1 antibody. This work was supported by NICHD grant RO1 38353 (S.A.C.) and by a grant from the Tri-Institutional Stem Cell Initiative funded by the Starr Foundation.

References

Aoki, F., Worrad, D. M. and Schultz, R. M. (1997). Regulation of transcriptional activity during the first and second cell cycles in the preimplantation mouse embryo. *Dev. Biol.* **181**, 296-307.

Bachvarova, R. and De Leon, V. (1977). Stored and polysomal ribosomes of mouse ova. *Dev. Biol.* **58**, 248-254.

Bachvarova, R., De Leon, V. and Spiegelman, I. (1981). Mouse egg ribosomes: evidence for storage in lattices. *J. Embryol. Exp. Morphol.* **62**, 153-164.

Bellier, S., Chastant, S., Adenot, P., Vincent, M., Renard, J. P. and Bensaude, O. (1997). Nuclear translocation and carboxyl-terminal domain phosphorylation of RNA polymerase II delineate the two phases of zygotic gene activation in mammalian embryos. *EMBO J.* **16**, 6250-6262.

Brower, P. T. and Schultz, R. M. (1982). Biochemical studies of mammalian oogenesis: possible existence of a ribosomal and poly(A)-containing RNA-protein supramolecular complex in mouse oocytes. *J. Exp. Zool.* **220**, 251-260.

Bultman, S. J., Gebuhr, T. C., Pan, H., Svoboda, P., Schultz, R. M. and Magnuson, T. (2006). Maternal BRG1 regulates zygotic genome activation in the mouse. *Genes Dev.* **20**, 1744-1754.

Burns, K. H., Viveiros, M. M., Ren, Y., Wang, P., DeMayo, F. J., Frail, D. E., Eppig, J. J. and Matzuk, M. M. (2003). Roles of NPM2 in chromatin and nucleolar organization in oocytes and embryos. *Science* **300**, 633-636.

Capco, D. G., Gallicano, G. I., McGaughey, R. W., Downing, K. H. and Larabell, C. A. (1993). Cytoskeletal sheets of mammalian eggs and embryos: a lattice-like network of intermediate filaments. *Cell Motil. Cytoskel.* **24**, 85-99.

Christians, E., Davis, A. A., Thomas, S. D. and Benjamin, I. J. (2000). Maternal effect of Hsf1 on reproductive success. *Nature* **407**, 693-694.

Conover, J. C., Temeles, G. L., Zimmermann, J. W., Burke, B. and Schultz, R. M. (1991). Stage-specific expression of a family of proteins that are major products of zygotic gene activation in the mouse embryo. *Dev. Biol.* **144**, 392-404.

Davidson, E. R. (1986). In *Gene Activity in Early Development*. Orlando, FL: Academic Press.

Esposito, G., Vitale, A. M., Leijten, F. P., Strik, A. M., Koonen-Reemst, A. M., Yurttas, P., Robben, T. J., Coonrod, S. and Gossen, J. A. (2007). Peptidylarginine deiminase (PAD) 6 is essential for oocyte cytoskeletal sheet formation and female fertility. *Mol. Cell. Endocrinol.* **273**, 25-31.

Garcia, R. B., Pereyra-Alfonso, S. and Sotelo, J. R. (1979). Protein-synthesizing machinery in the growing oocyte of the cyclic mouse. A quantitative electron microscopic study. *Differentiation* **14**, 101-106.

Hesketh, J. E. and Pryme, I. F. (1991). Interaction between mRNA, ribosomes and the cytoskeleton. *Biochem. J.* **277**, 1-10.

Hovland, R., Hesketh, J. E. and Pryme, I. F. (1996). The compartmentalization of protein synthesis: importance of cytoskeleton and role in mRNA targeting. *Int. J. Biochem. Cell Biol.* **28**, 1089-1105.

Ma, J., Zeng, F., Schultz, R. M. and Tseng, H. (2006). Basonuclin: a novel mammalian maternal-effect gene. *Development* **133**, 2053-2062.

McGaughey, R. W. and Capco, D. G. (1989). Specialized cytoskeletal elements in mammalian eggs: structural and biochemical evidence for their composition. *Cell Motil. Cytoskel.* **13**, 104-111.

Oh, B., Hwang, S. Y., Solter, D. and Knowles, B. B. (1997). Spindlin, a major maternal transcript expressed in the mouse during the transition from oocyte to embryo. *Development* **124**, 493-503.

Oh, B., Hwang, S., McLaughlin, J., Solter, D. and Knowles, B. B. (2000). Timely translation during the mouse oocyte-to-embryo transition. *Development* **127**, 3795-3803.

Palancade, B. and Bensaude, O. (2003). Investigating RNA polymerase II carboxyl-terminal domain (CTD) phosphorylation. *Eur. J. Biochem.* **270**, 3859-3870.

Ratnam, S., Mertineit, C., Ding, F., Howell, C. Y., Clarke, H. J., Bestor, T. H., Chaillet, J. R. and Trasler, J. M. (2002). Dynamics of Dnmt1 methyltransferase expression and intracellular localization during oogenesis and preimplantation development. *Dev. Biol.* **245**, 304-314.

Roth, S. Y., Denu, J. M. and Allis, C. D. (2001). Histone acetyltransferases. *Annu. Rev. Biochem.* **70**, 81-120.

Schultz, R. M., Davis, W., Jr, Stein, P. and Svoboda, P. (1999). Reprogramming of gene expression during preimplantation development. *J. Exp. Zool.* **285**, 276-282.

Spector, D. (1998). *Cells, A Laboratory Manual*. Cold Spring Harbor, New York: Cold Spring Harbor Press.

Sternlicht, A. L. and Schultz, R. M. (1981). Biochemical studies of mammalian oogenesis: kinetics of accumulation of total and poly(A)-containing RNA during growth of the mouse oocyte. *J. Exp. Zool.* **215**, 191-200.

Sun, Q. Y. and Schatten, H. (2006). Regulation of dynamic events by microfilaments during oocyte maturation and fertilization. *Reproduction* **131**, 193-205.

Tong, Z. B., Gold, L., De Pol, A., Vanevski, K., Dorward, H., Sena, P., Palumbo, C., Bondy, C. A. and Nelson, L. M. (2004). Developmental

expression and subcellular localization of mouse MATER, an oocyte-specific protein essential for early development. *Endocrinology* **145**, 1427-1434.
Wang, Q. and Latham, K. E. (1997). Requirement for protein synthesis during embryonic genome activation in mice. *Mol. Reprod. Dev.* **47**, 265-270.
Wassarman, P. M. and Josefowicz, W. J. (1978). Oocyte development in the mouse: an ultrastructural comparison of oocytes isolated at various stages of growth and meiotic competence. *J. Morphol.* **156**, 209-235.
Worrad, D. M., Turner, B. M. and Schultz, R. M. (1995). Temporally restricted spatial localization of acetylated isoforms of histone H4 and RNA polymerase II in the 2-cell mouse embryo. *Development* **121**, 2949-2959.
Wright, P. W., Bolling, L. C., Calvert, M. E., Sarmento, O. F., Berkeley, E. V., Shea, M. C., Hao, Z., Jayes, F. C., Bush, L. A., Shetty, J. et al. (2003). ePAD, an oocyte and early embryo-abundant peptidylarginine deiminase-like protein that localizes to egg cytoplasmic sheets. *Dev. Biol.* **256**, 73-88.
Wu, X., Viveiros, M. M., Eppig, J. J., Bai, Y., Fitzpatrick, S. L. and Matzuk, M. M. (2003). Zygote arrest 1 (Zar1) is a novel maternal-effect gene critical for the oocyte-to-embryo transition. *Nat. Genet.* **33**, 187-191.
Zamboni, L. (1970). Ultrastructure of mammalian oocytes and ova. *Biol. Reprod.* **2 Suppl.**, 44-63.